

**Structural Shear behavior of Composite Box beams
using advanced innovated materials**

ABSTRACT

The Paper opens a new conception of shear behaviour of box concrete beams reinforced by composite fabrics. For this purpose, stirrups, wire meshes as shear reinforcement were used. Seven box section concrete beams were tested using two-point loading system. Beams with tensar wire mesh exhibited increasing in ultimate failure load, shear capacity and deflection with respect to beams with reference & glass fiber wire mesh. Nonlinear finite element analysis was conducted using Ansys 14.5 to verify the experimental test program. Sensible agreement was found between the experimental and numerical results.

Keywords: [Composite structures, box beams, shear stress, composite materials, glass fiber wire mesh, tensar wire mesh, nonlinear finite element analysis (NLFEA), Ansys 14.5]

1. INTRODUCTION

Wire meshes were used to belay the new system and to improve its performance [1,2]. Ferrocement is named as wire mesh reinforcement. The flexure behavior of wire meshes had been studied and noticed to be nearly to reinforced concrete members [3,6]

A1-Sulaimani et al [7,8] recommended studying the behavior of composite ferrocement beams under transversal shear stress.

Mansur & Ong [9] had studied the shear behaviour of rectangular ferrocement beams. Ferrocement rectangular beams were found to be critical to shear collapse at comparatively high V_f and f_c .

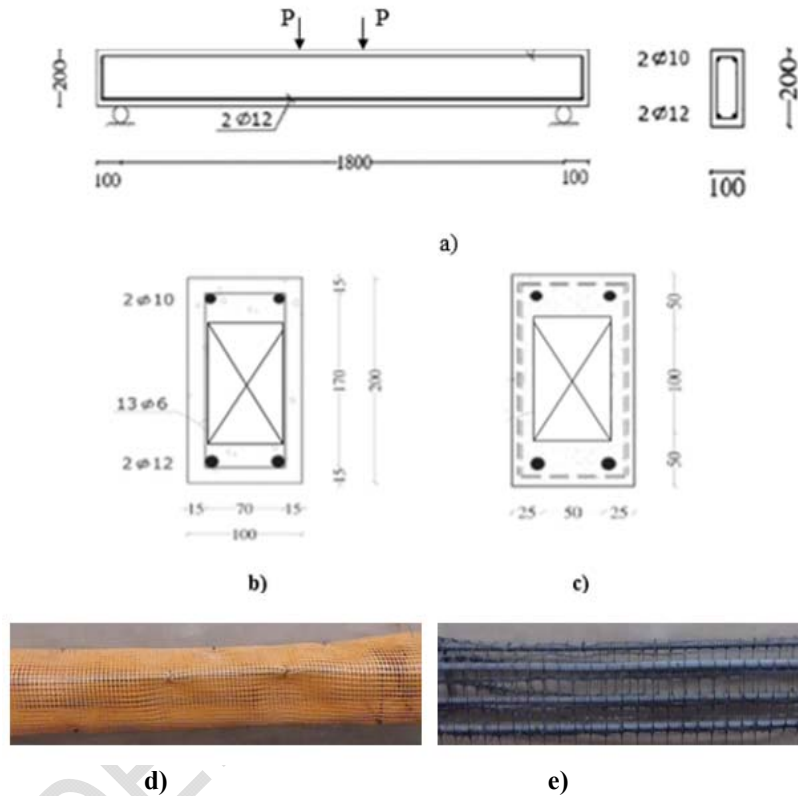
El-Sayed & Erfan [10] improved the shear behaviour of ferrocement composite beams. Test results showed that beams with expanded wire mesh exhibited some amount of increase in shear capacity with respect to beams with reference & welded wire mesh.

2. EXPERIMENTAL PROGRAM

The experimental work was done to investigate the general behaviour, cracks pattern, shear stresses and the ultimate capacity of the reinforced concrete box beam reinforced by composite fabrics. The experimental program consisted of seven composite box beams having the cross-sectional dimensions of 100 mm x200 mm and 1800 mm long were cast and tested until failure. All specimens were reinforced with the same longitudinal bars in tension and compression. The specimens were tested using two-point loading. The reinforcing bars were designed and detailed, and the bearing pad was proportioned such that the flexural, anchorage and bearing modes of failure were avoided. The concrete mix for the test specimens was designed to obtain compressive strength at 28days age of 30 MPa. The mix proportions were 2 sand: 1 cement, water cement ratio was 0.3 and 1.5% super plasticizer by weight of cement. The concrete slump was found to be 130 mm and a density of 2500 Kg/m³. All specimens were tested using compression testing machine of capacity 2000 KN.

43 **2.1 Preparation of Specimens and samples description**

44 The experimental program consists of seven box beams with the same geometry and steel
 45 reinforcement details as shown in Fig. 1, were prepared for testing under concentric loads. The control
 46 specimen was box section beam reinforced using 2Ø12 in tensions and 2Ø10 in compression and
 47 13Ø6 as stirrups. The other six box beams haven't stirrups but using glass fiber and tenasr
 48 composite instead of stirrups. The first group consists of three beams Box1-1, Box2-1 and Box3-1
 49 which reinforced using one, two and three layers of glass fiber wire mesh respectively. Second group
 50 for Box1-2, Box2-2 and Box3-2 which reinforced using one, two and three tenasar wire mesh instead
 51 of stirrups respectively as described in Table 1.
 52



53
 54
 55 Fig.1: beams geometric shape and reinforcement details, a) Control specimen; b) Cross-section of
 56 beam with steel stirrups; c) Cross-section of beam glass fiber wire mesh or tenasar layer mesh; d)
 57 Beams with glass fiber wire mesh; e) Beams with tenasar wire mesh
 58

59
 60 Table 1: Box beams specimen's descriptions and notations

Series	Specimen No.	Specimens description	Reinf. Tension	Compression	Vr. Stirrups
Control	BOX1	Control specimen	2Ø12	2 Ø10	13Ø6
Group 1 "Glass fiber wire mesh"	BOX1-1	One-layer glass fiber	2 Ø12	2 Ø10	-
	BOX2-1	Two-layer glass fiber	2 Ø12	2 Ø10	-
	BOX3-1	Three-layer glass	2 Ø12	2 Ø10	-

Group 2 “Tensar wire mesh”	BOX1-2	fiber One-layer tensar	2φ12	2 φ10	-
	BOX2-2	Two-layer tensar	2 φ12	2 φ10	-
	BOX3-2	Three-layer tensar	2 φ12	2 φ10	-

61

62 **2.2 Characteristics of Materials**

63

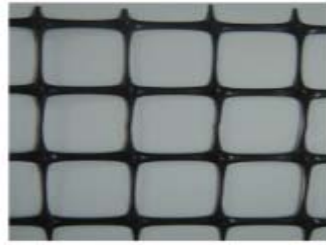
64 The concrete mix contents utilized for the experimental program was summarized in Table 2 which
65 gives concrete characteristic strength of 30 MPa. The reinforced steel obtained from El-Dekhiela
66 factory was $f_y=360$ MPa (for deformed bars) and $f_y=240$ MPa (for plain bars). Fig.2 showed either
67 tensar or fiber glass wire meshed used. Table 3 summarized the properties of both wire meshes as per
68 manufacturer. The beams were casted in a horizontal position and the vibrated concrete placed
69 compacted in wooden molds.

70

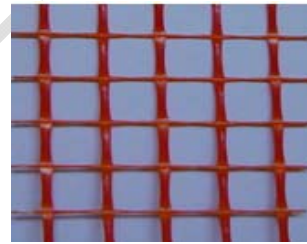
71 Table 2: The Contents of Concrete Mixture

72

Contents	Amount	73
Cement	350 K_g/m^3	74
Sand	700 K_g/m^3	75
Aggregate (1)	540 K_g/m^3	76
Aggregate (2)	620 K_g/m^3	77
Water	162.5 L/m^3	78
Admix	2 L/m^3	79
		80
		81



82 a)



83 b)

84

85

84 Fig.2: Configurations of composites materials; a) Polyethylene (Tensar) wire mesh, b) Fiber
85 glass wire mesh

86

87

86 Table 3: Mechanical properties of tensar and fiber glass wire meshes

Polyethylene (Tensar) wire mesh		Glass fiber wire mesh	
Dimensions size	6.0 x 8.0 mm	Dimensions size	12.5 x 11.5 mm
Weight	725 gm/m^2	Weight	123 gm/m^2
Sheet Thickness	3.30 mm	Sheet Thickness	0.66 mm
Yield Stress	260 N/mm^2	Yield Stress	230 N/mm^2
Young's modulus	100000	Young's modulus	80000

88
89
90
91
92
93
94
95
96

2.3 Test setup

The composite box beams were tested under two-point load testing machine of maximum capacity of 2000 KN with 1800mm effective span and 750mm shear span and 300mm load distance as shown in Fig. 3. Load was affective at 20 KN increments on the tested specimens. The LVDT and dial gages were used of high accuracy to measure the deflections and strains for steel and concrete. The load still increased till failure load and maximum displacements.

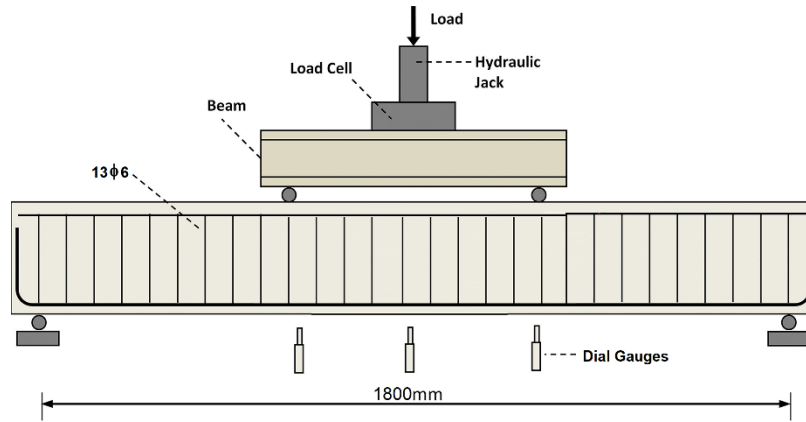


Fig. 3: Test set up schematic

97
98
99
100
101
102
103
104
105
106
107
108
109
110

3. RESULTS AND DISCUSSION

Test results include the load carrying capacity and displacement in concrete box beams. The cracks propagation during the tests was recorded. The crack initialization in the specimens reinforced using wire meshes was developed however, at later stages with respect to the control specimen. Also, the cracks lengths and widths decreased in the specimens reinforced with either glass fiber or tensar wire meshes as compared with the control specimen.

111
112
113
114
115
116
117
118
119
120
121

3.1 Cracking

The first crack for all tested box beams were developed horizontally under the load pint in the mid span. Control specimen cracks observed at a load of 7.5 KN. For specimens BOX1-1, BOX2-1 and BOX3-1, a higher ultimate load was recorded 1.04, 1.1 and 1.25 times than control one respectively. The diagonal cracking initiated in the Control Specimen; BOX1 increased in length and width until failure at load of 42.5 KN. For specimens BOX1-2, BOX2-2 and BOX3-2, a higher ultimate load was recorded 1.02, 1.12 and 1.18 times than control specimen respectively. Using fiber glass wire mesh and tensar wire mesh instead of stirrups was enhanced the crack pattern for box beams as shown in Fig. 4.

122
123



a)

124
125



b)

126
127



c)

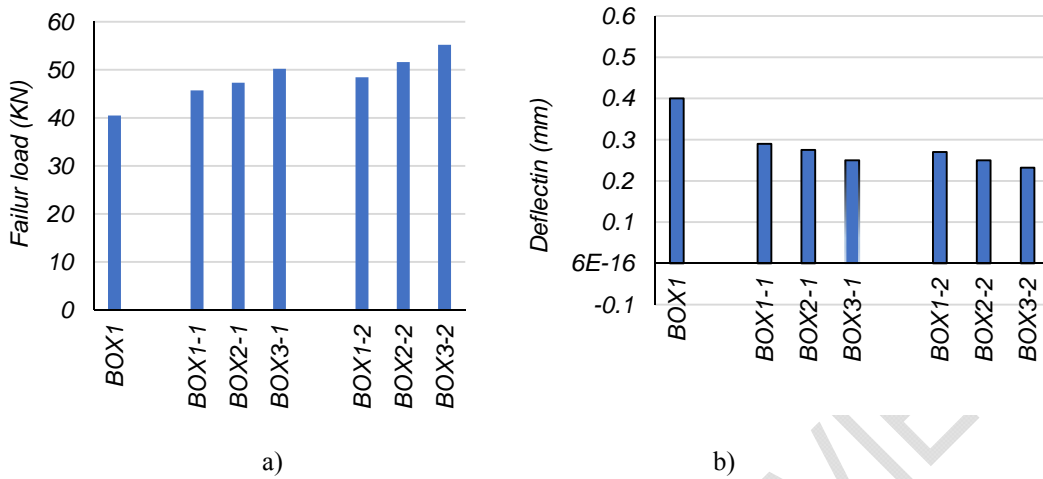
128 Fig.4: Sample of crack pattern; a) control specimen; b) glass fiber wire mesh; c)
129 Polyethylene (tensar) wire mesh.
130

131 3.2 Ultimate load Capacity

132 The load carrying capacity is differ from one box beam to another according to its reinforcement and
133 using tensar and glass fiber wire mesh instead of steel stirrups. For the control specimen, the ultimate
134 failure load was 40.5 KN. The first group which reinforced using glass fiber wire mesh recorded
135 failure loads of 45.7, 47.3 and 50.2 KN for BOX1-1, BOX2-1 and BOX3-1 respectively with
136 enhancement ratio with respect to the control beam of 12.8%, 16.8% and 23.9% respectively. This
137 enhancement related to layers number of glass fiber wire mesh used in reinforcement as shown in
138 Table 4. For the second group which reinforced using Polyethylene (tensar) wire mesh of different
139 layers number of BOX1-2, BOX2-2 and BOX3-2. The experimental failure loads were 48.44, 51.6
140 and 55.2 KN with enhancement ratio of 19.6%, 27.4% and 36.3% for BOX1-2, BOX2-2 and BOX3-2
141 respectively. Observing that using three layers of either glass fiber or tensar wire mesh recorded the
142 highest load and enhancement in carrying capacity. It is noticed that the effect of using tensar wire
143 mesh has the major effect in load carrying capacity as shown in Table 4 and Fig. 5.
144
145
146

Table 4: Experimental testing results

Series	Specimen No.	Failure load (KN)	% Of enhancement in load	Deflection (mm) at failure load
Control	BOX1	40.5	---	0.40
Group 1 "glass fiber wire mesh"	BOX1-1	45.7	12.8	0.290
	BOX2-1	47.3	16.8	0.278
	BOX3-1	50.2	23.9	0.250
Group 2 "Polyethylene (tensar) wire mesh"	BOX1-2	48.4	19.6	0.270
	BOX2-2	51.6	27.4	0.250
	BOX3-2	55.2	36.3	0.230



148
149
150

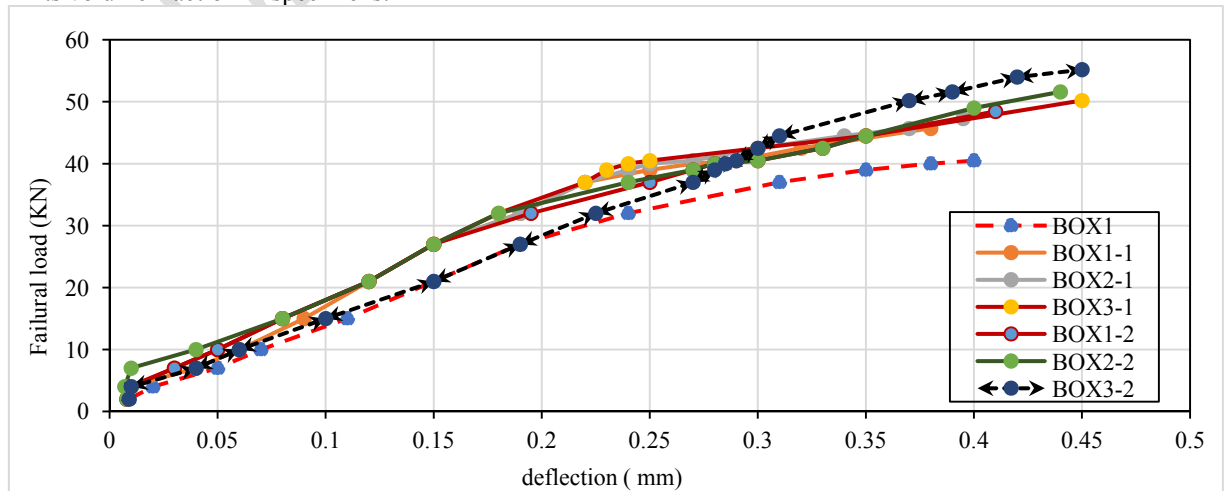
151 Fig. 5: comparison between experimental results; a) failure load (KN); b) deflection (mm) at ultimate
152 load of control specimen

153
154

3.3 Experimental ultimate deflection

155 As shown in Table 4 and Fig. 5.b and Fig. 6 the experimental deflection recorded for different
156 specimens with different reinforcement types. The deflection recorded for the control specimen was
157 0.40 mm at failure load. For group one which reinforced with glass fiber wire mesh, the maximum
158 deflection at failure load was 0.38, 0.39 and 0.45 mm but at the same failure load of the control, it was
159 0.29, 0.278 and 0.25 mm respectively which is lower than the control specimen. This indicates the
160 effect of glass fiber wire mesh in decreasing the deflection with average ratio of 32.0%. For group two
161 which reinforced with Polyethylene (tensar) wire mesh, the maximum deflection at failure load was
162 0.41, 0.44 and 0.45 mm which is higher than the control specimen but if the deflection recorded at
163 specimens BOX1-2, BOX2-2 and BOX3-2 at failure load of control specimen which was 0.27, 0.25
164 and 0.23 mm respectively. This indicates the effect of tensar wire mesh in decreasing the deflection
165 with average ratio of 37.5%. This ratio indicates that the tensar wire mesh has the best effect in
166 decrease the deflection.

167 The decrease in ultimate deflection of group one and two is mainly due to increase in number of glass
168 fiber or tensar wire mesh layers used in reinforcement instead of steel stirrups which lead to increase
169 in its volume fraction in specimens.



170

171
172
173
174
175
176
177
178
179
180
181
182
183
184
185
186
187
188
189
190
191
192
193
194
195
196
197
198
199
200
201
202
203
204
205
206
207
208
209
210
211
212
213

Fig. 6: Experimental load deflection curve

3.4 Ductility and energy absorption

Ductility is defined as the ratio between the deflections at ultimate load to the deflection at the first crack load but the energy absorption is the total area under the load deflection curve. The ductility recorded an average ratio for different specimens of 5.66. A progressive increase of energy absorption which represents the specimen toughness with volume friction percentage and ductility was observed. For the control specimen BOX1 the energy absorption recorded 285.6 KN.mm, compared this value with the recorded for different series it shows good enhancement. For all series the enhancement percentage varies between 99.6% and 129%. The smallest enhancement was at specimen BOX1-2 which use one glass fiber layer instead of stirrups due to the weak properties of the used type of layer but the highest enhancement was in BOX3-2 which used three tensar layers wire mesh. Finally using reinforced with various types of composite materials were developed with high ultimate loads, crack resistance, better deformation characteristics, high durability and energy absorption properties, which are very useful for dynamic effect.

3.5 shear stress

The obtained shear stresses are obtained according to the ECP203/207 [11]. For the control specimen BOX1 the shear stress was 2.25 MPa. For the first group box beams BOX1-1, BOX2-1 and BOX3-1 the shear stresses were 2.53, 2.62 and 2.78 MPa respectively with an enhancement ratio of 12.5%, 16.5% and 23.5% respectively with respect to the control specimen. The second group which used Polyethylene (tensar) wire mesh instead of stirrups, the shear stresses was 2.69MPa, 2.86 MPa and 3.06 MPa for BOX1-2, BOX2-2 and BOX3-2 respectively. The enhancement in this group with respect to the control specimen was 19.5%, 27.1% and 36.0% respectively which is relatively more than the group used the glass fiber wire mesh.

4. Non-linear finite element analysis study

NLFEA study was done to verify the obtained experimental results. The groups studied were as shown in Table 1 which divided in to control specimen and other two groups. Group one which used glass fiber wire mesh instead of steel stirrups with different number of layers. The second group used Polyethylene (tensar) wire mesh instead of steel stirrups. These specimens were modeled and analyzed using ANSYS 14.5 [12] program.

4.1 specimens modeling

NLFEA was carried out to estimate the behavior of composite box beams as shown in Fig. 7. The discussed behavior included the ultimate capacity, deflection, shear stresses and crack pattern for each specimen.

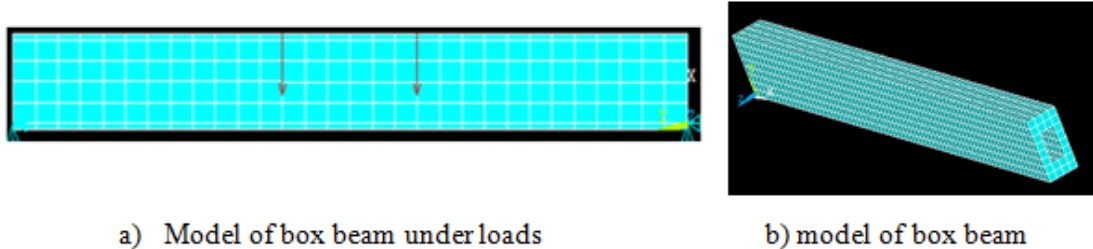


Fig. 7: NLFEA model of examined box beams

214
215
216

217 **4.1.1 Model Elements Types**

218 Solid 65 represent the concrete element which represents the stress strain curve for concrete in
219 compression and the other properties of it represent the concrete strength in tension. The other used
220 element was LINK 8 3-D to represent the steel bars with its strength and steel stirrups. The composite
221 materials of glass fiber or Polyethylene (tensar) wire mesh was represented by calculating the
222 volumetric ratio of it in the concrete element using its properties by calculating the ratio of steel to
223 concrete in each element as shown in Fig. 8. Each material has its X, Y and Z coordinates and has its
224 orientation angle and its reinforcement in wire mesh smeared element.

225

226

227

228

229

230

231

232

233

234

235

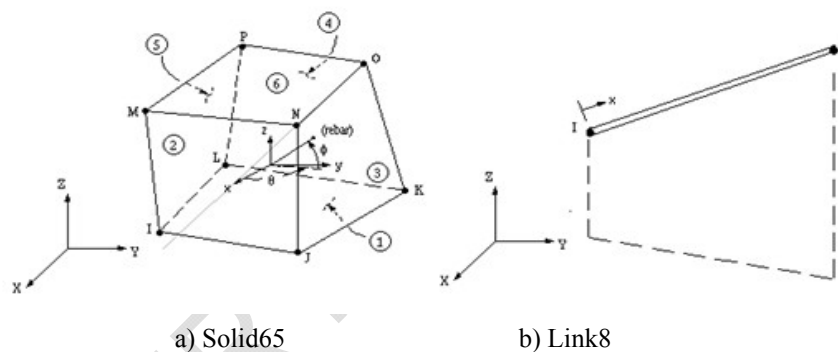


Fig. 8: Geometry of element types

236

237

238

239

240

241

242

243

244

245

246

247

248

249

250

251

252

253

4.1.2 Modelling Material properties

The mechanical properties for element SOLID65 and LINK 8 which represent concrete and steel reinforcement respectively was Elastic modulus of elasticity ($E_c = 4400\sqrt{f_{cu}} = 24100 \text{ N/mm}^2$) and Poisson's ratio ($\nu=0.3$), but Yield stress ($f_y=360 \text{ N/mm}^2$ & $f_{yt}=240 \text{ N/mm}^2$) with Poisson's ratio ($\nu=0.2$) [11].

For the element which represents the composite properties for glass fiber wire mesh are as the given. The glass fiber wire mesh which has diamond size is 12.5 x 11.5mm with thickness of 0.66 mm, the volumetric ratio of one layer of glass fiber mesh ($V1=0.00872$), two layers was ($V1=0.0174$) but for the three layers of glass fiber the volumetric ratio is ($V1=0.02616$). For the Polyethylene (tensar) layers the size of opening is 6.0 x 8.0mm with wires of diameter 3.3 mm. The volumetric ratio of one layer of tensar mesh ($V1=0.14800$), two layers was ($V1=0.29600$) but for the three layers the volumetric ratio of three layer of tensar mesh ($V1=0.44400$).

254

255 4.2 Analytical Results and Discussion

256

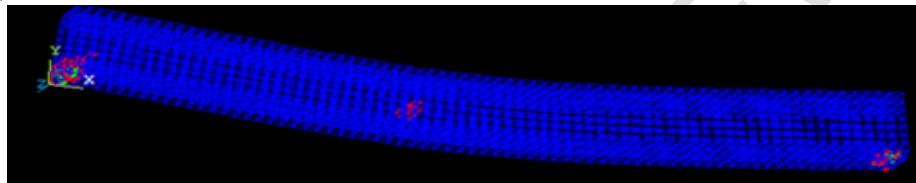
257 The finite element program presents the nonlinear response of the box beams specimens. Loading was
258 incrementally increased until failure and divergence occurs which lead to failure. The finite element
259 results represent the cracks patterns, failure load, deflection, shear stresses and yielding of steel as
260 shown in Table 5.

261

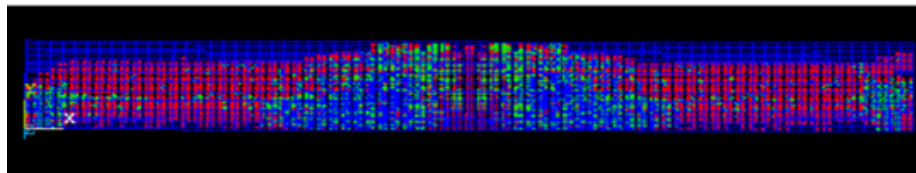
262 4.2.1 Cracking

263

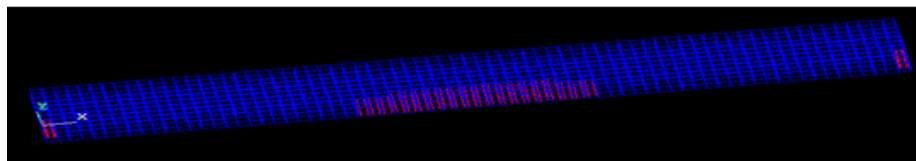
264 The first crack in the entire tested box beam was slightly inclined crack developed under the load pint
265 in the mid span. This first crack in the control specimen observed at a load of 4.0 KN. For specimens
266 BOX1-1, BOX2-1 and BOX3-1, it was recorded at a higher load being 1.2, 1.15 and 1.05 times that of
267 the Control Specimen; BOX1, respectively. The cracking initiated in the Control Specimen; BOX1
268 increased in numbers until failure at load of 36.0 KN. For specimens BOX1-2, BOX2-2 and BOX3-2,
269 it was recorded at a higher load with respect to control specimen being 0.95, 1.05 and 1.12 times that
270 of the control specimen; BOX1, respectively. Using the fiber glass wire mesh and Polyethylene
271 (tenasr) wire mesh instead of stirrups enhance the crack pattern for box section beam as shown in Fig.
272 9.C.



a)



b)



c)

273

274 **Fig.9: Sample of crack pattern for control specimen; a) first cracks; b) cracks at**
275 **failure; c) sample of cracks for specimens in group 1 and 2.**

276

277 4.2.2 Ultimate Failure Load

278 The load carrying capacity is differing from one box section to another according to its reinforcement
279 and using glass fiber wire mesh and polyethylene (tenasr) wire mesh instead of steel stirrups. For the
280 control specimen BOX, the ultimate failure load was 36.0 KN. The first group which reinforced using
281 glass fiber wire mesh recorded failure loads of 42.8, 44.2 and 48.3 KN for BOX1-1, BOX2-1 and
282 BOX3-1 respectively with enhancement ratio with respect to the control beam of 18.8%, 22.8% and
283 34.1% respectively. This enhancement related to number of fiber glass wire mesh used in
284 reinforcement as shown in Table 5. For the second group which reinforced using tenasr wire mesh of
285 different layers number of BOX1-2, BOX2-2 and BOX3-2. The NLFE failure loads were 45.7, 49.2

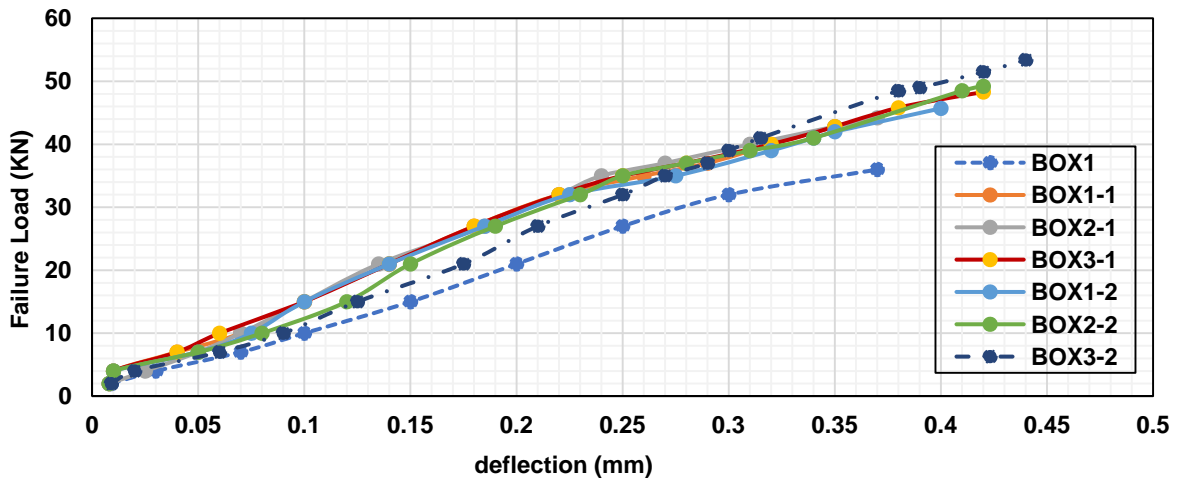
286 and 53.4 KN with enhancement ratio of 26.9%, 36.7% and 48.3% for BOX1-2, BOX2-2 and BOX3-2
 287 respectively. Observing that using three layers of either glass fiber or tensar wire mesh recorded the
 288 highest load and enhancement in carrying capacity. It is noticed that the effect of using tensar wire
 289 mesh has the major effect in load carrying capacity as shown in Table 5 and Fig. 10.
 290

291 **4.2.3 Analytical Ultimate deflection**

292 The analytical deflection recorded for different specimens with different reinforcement types is
 293 recorded as in Table 5 and Fig. 10 and Fig. 11. The deflection of the control specimen was 0.37 mm at
 294 failure load. For group one which reinforced with glass fiber wire mesh, the maximum deflection at
 295 failure load was 0.35, 0.37 and 0.42 mm but at the same load of the control specimen it was 0.26, 0.24
 296 and 0.25mm respectively which is lower than the control specimen. This indicates the effect of glass
 297 fiber wire mesh in decreasing the deflection with average ratio of 29.7%.

298 For group two which reinforced with Polyethylene (tensar) wire mesh, the maximum deflection at
 299 failure load was 0.40, 0.42 and 0.415 mm which is higher than the control specimen but if the
 300 deflection recorded at specimens BOX1-2, BOX2-2 and BOX3-2 at failure load of control specimen
 301 which was 0.265, 0.250 and 0.270 mm respectively. This indicates the effect of tensar wire mesh in
 302 decreasing the deflection with average ratio of 29.8%. This ratio indicates that the tensar wire mesh
 303 has relatively best effect in decrease the deflection.

304 The decrease in ultimate deflection of group one and two is mainly due to increase in number of glass
 305 fiber or tensar wire mesh layers used in reinforcement which lead to increase in its volume fraction in
 306 specimens.
 307



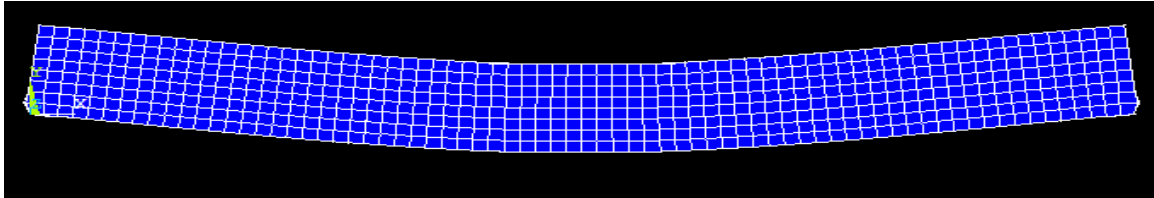
308
 309
 310 Fig. 10: NLFE load deflection curves
 311
 312

313 Table 5: NLFEA Analytical Results

Series	Specimen No.	Failure load (KN)	% Of enhancement in Deflection load	(mm) at failure load
Control	BOX1	36.0	---	0.370
Group 1 "glass fiber wire mesh"	BOX1-1	42.8	18.8	0.370
	BOX2-1	44.2	22.8	0.350

			BOX3-1	48.3	34.1	0.420
Group 2 (tensar) wire mesh”	“Polyethylene		BOX1-2	45.7	26.9	0.400
			BOX2-2	49.2	36.7	0.410
			BOX3-2	53.4	48.3	0.415

314
315



316
317
318
319
320

Fig.11 Typical deformation of NLFEA deflection for box beams

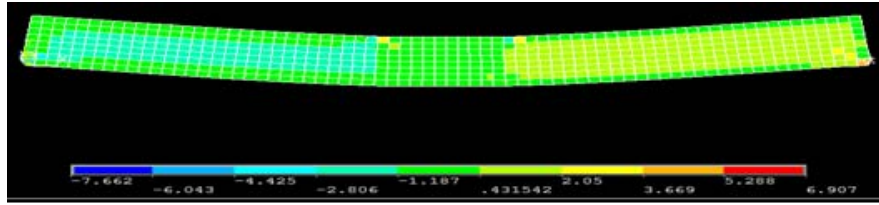
4.2.4 Ductility and energy absorption

321 A progressive increase of energy absorption which represents the specimen toughness with volume
322 friction percentage and ductility was observed. For the control specimen BOX1 the energy absorption
323 recorded 249.9 KN.mm, compared this value with the recorded for different series it shows good
324 enhancement. For all series the enhancement percentage varies between 45.1% and 159%. The
325 smallest enhancement was at specimen BOX1-2 which use one Polyethylene (tensar) layer instead of
326 stirrups due to the properties of the used type of layer but the highest enhancement was in BOX3-1
327 which used three tensar layers wire mesh which agreed with the results. Finally using composite
328 materials were developed with high ultimate loads, crack resistance, better deformation
329 characteristics, high durability and energy absorption properties, which are very useful for dynamic
330 effect.

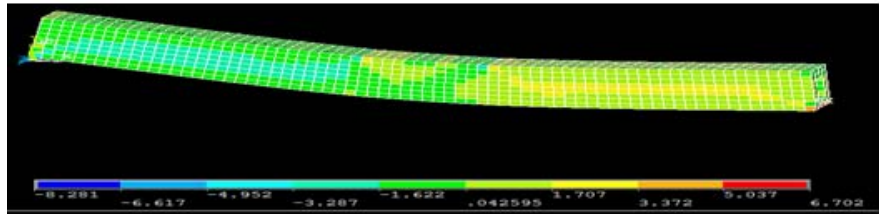
331
332

4.2.5 Shear stresses

333 The obtained shear stresses are obtained according to the obtained results from the NLFEA as shown
334 in Fig.12. For the control specimen BOX1 the shear stress was 2.0 MPa. For the first group box
335 beams BOX1-1, BOX2-1 and BOX3-1 the shear stresses were 2.37, 2.45 and 2.68 MPa respectively
336 with an enhancement ratio of 18.5%, 22.5% and 34.0% respectively with respect to the control
337 specimen. The second group which used the Polyethylene (tensar) wire mesh instead of stirrups, the
338 shear stresses was 2.53 MPa, 2.73 MPa and 2.96 MPa for BOX1-2, BOX2-2 and BOX3-2
339 respectively. The enhancement in this group with respect to the control specimen was 26.5%, 36.5%
340 and 48.0% respectively which is relatively more than the group used the glass fiber wire mesh.



a)



b)

341 Fig.12 NLFEA Shear Stresses; a) Shear stresses for BOX1; b) Sample of shear stresses for different
 342 specimens
 343
 344

345 5. Comparison between experimental and NLFEA results

346
 347 These comparisons aim to ensure the NLFEA models are available and suitable to exhibit the
 348 response of composite box beams. There are seven finite element models were compared with seven
 349 experimental specimens in term of ultimate load, ultimate deflection and crack patterns.
 350

351 5.1 Ultimate failure load

352
 353 There was an acceptable agreement between the experimental failure load and the analytical failure
 354 load obtained from NLFE program as shown in Table 6 and Fig.13. The ratio between the NLFE
 355 failure loads to the experimental failure load varies between 0.90 to 0.96 with an average ratio of 0.94.
 356 The ratio of $P_{u\ NLFE} / P_{u\ Exp}$ for control specimen was 0.90 but for the specimens in group one, it was
 357 0.93, 0.94 and 0.96 for BOX 1-1, BOX2-1 and BOX3-1 respectively.
 358 For the second group this ratio was 0.94, 0.95 and 0.96 for BOX 1-2, BOX2-2 and BOX3-2
 359 respectively. This shows that the NLFEA gives the aim of the studied parameters in face of load
 360 carrying capacity.
 361
 362

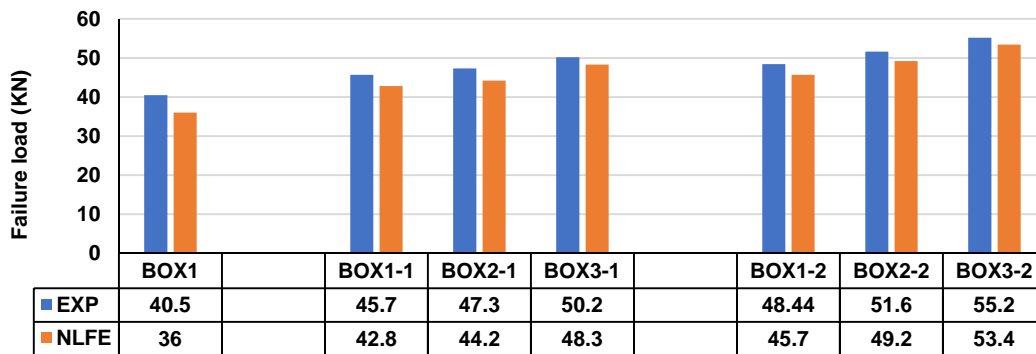
363 5.2 Ultimate Deflection

364
 365 Fig. 14 showed the load deflection curves for all box beams in phase of experimental and NLFE
 366 obtained results. The recorded deflection for experimental and NLFE analysis showed an agreement
 367 with respect to the deflection recorded for the control specimen as in Figure 15 and Table 6. The
 368 recorded ratio between $\Delta_{NLFE} / \Delta_{Exp}$ of 0.92 for the control specimen. For the first group this ratio
 369 recorded 0.92, 0.95 and 0.93 for BOX 1-1, BOX2-1 and BOX3-1 respectively but for BOX 1-2,
 370 BOX2-2 and BOX3-2, these ratios were 0.97, 0.95 and 0.92 respectively. These ratios showed that
 371 NLFE program provide an acceptable response in deflection as in Fig. 15.
 372
 373
 374
 375

376 Table 6: Comparison between experimental and NLFE Analysis

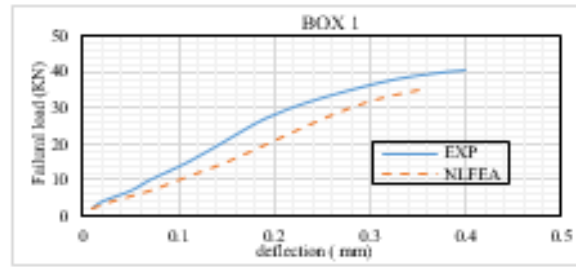
specimen	Failure load		Deflection		Shear stress		P_{ult} NLFEA/ $P_{ult exp}$	Δ_{ult} NLFE/ $\Delta_{ult exp}$	V_u NLFEA/ $V_u exp$
	P_{ult} (KN)		Δ_{ult} (mm)		V_u (MPa)				
	NLFEA	EXP	NLFEA	EXP	NLFEA	EXP			
BOX1	36.0	40.5	0.37	0.40	2.0	2.25	0.90	0.92	0.89
BOX1-1	42.8	45.7	0.35	0.38	2.37	2.53	0.93	0.92	0.94
BOX2-1	44.2	47.3	0.37	0.39	2.45	2.62	0.94	0.95	0.93
BOX3-1	48.3	50.2	0.42	0.45	2.68	2.78	0.96	0.93	0.96
BOX1-2	45.7	48.4	0.40	0.41	2.53	2.69	0.94	0.97	0.94
BOX2-2	49.2	51.6	0.42	0.44	2.73	2.86	0.95	0.95	0.95
BOX3-2	53.4	55.2	0.415	0.45	2.96	3.06	0.96	0.92	0.96

377
378

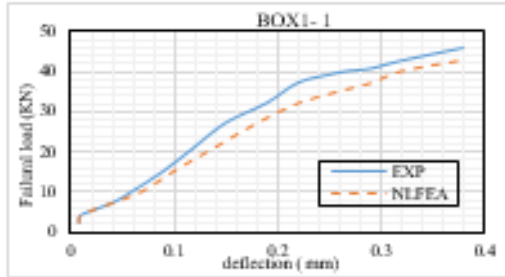


379
380

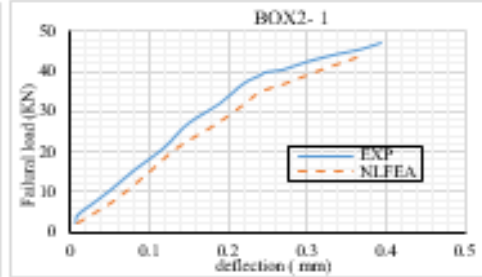
Fig. 13: Comparison between Exp. Failure load and NLFE failure load



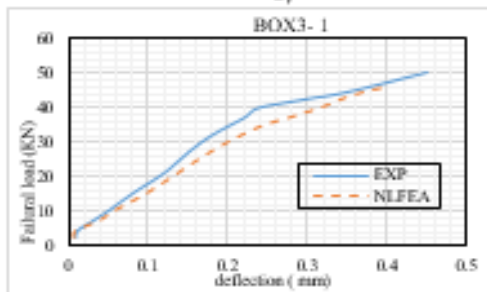
a)



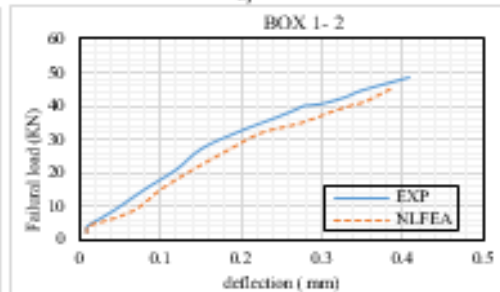
b)



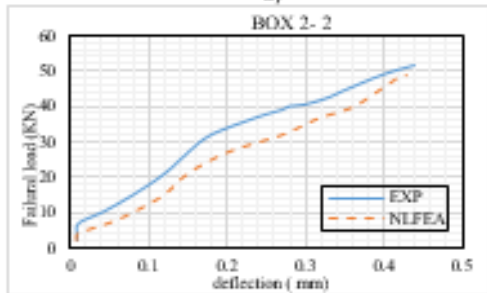
c)



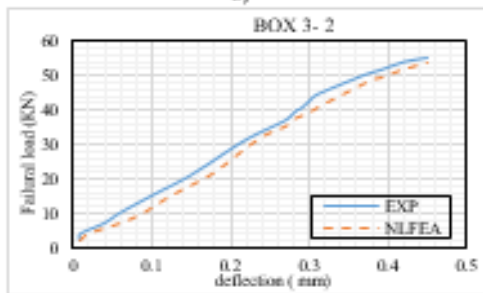
d)



e)



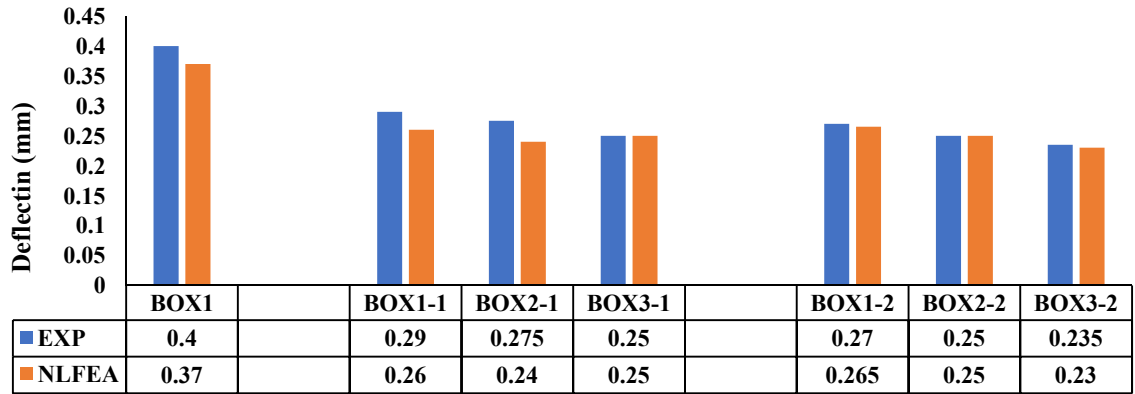
f)



g)

381
382
383
384
385

Fig. 14: Comparison between experimental and NLFEA load deflection curve; a) Control BOX1; b) BOX1-1; c) BOX2-1; d) BOX3-1; e) BOX1-2; f) BOX2-2; g) BOX3-1.

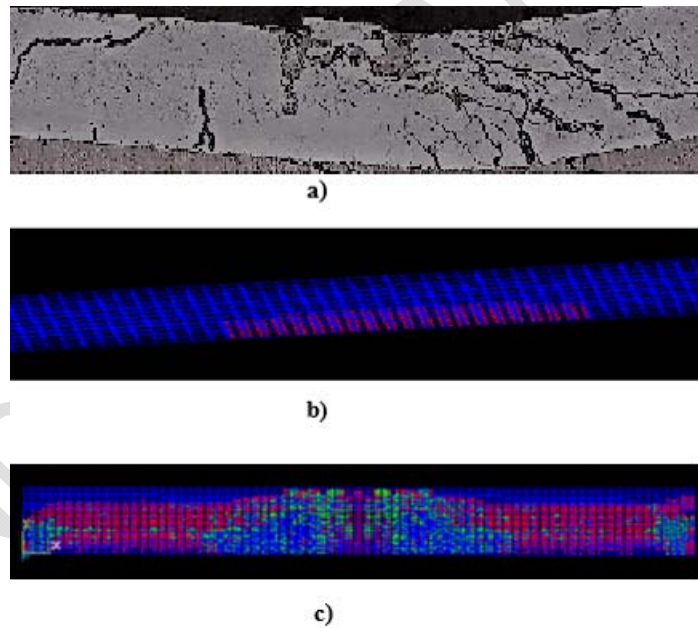


386
 387
 388
 389
 390
 391
 392
 393
 394
 395

Fig.15: Comparison between Exp. deflection and NLFE deflection at the failure load of control specimen.

5.3 Crack Patterns

The Fig. 16 indicate a comparison between the crack patterns experimentally and in NLFE analysis these cracks begins micro cracks and increased in length and width till failure



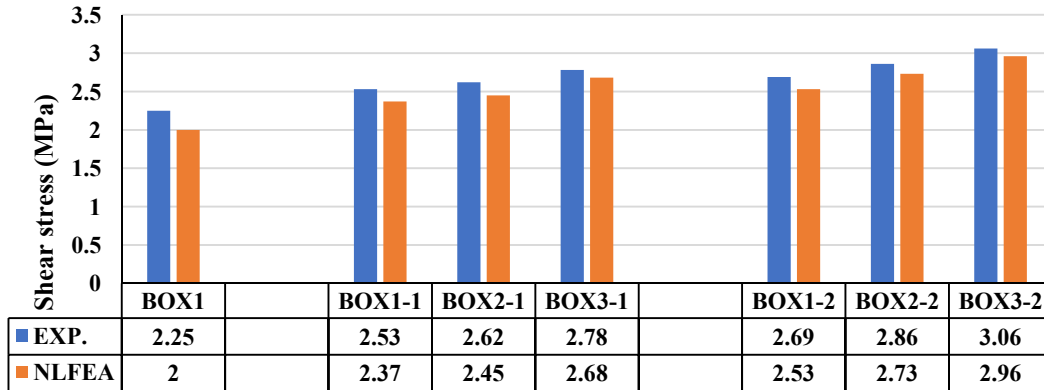
396
 397
 398
 399
 400
 401
 402
 403
 404
 405

Fig.16: Crack pattern for box beams; a) Experimental crack pattern; b) NLFE crack pattern; c) NLFE cracks till failure.

5.4 Shear Stresses

As the porpouse of this study was to discuss the shear stresses and the effect of using wire meshes in resist shear and cracks propagates. The experimental and NLFEA showed reasonable agreement in the obtained results as shown in Fig. 17 and Table 6. The ratio between the shear stresses from NLFEA and experimental test was 0.89 for control specimen, but for the group one which used glass fiber wire

406 mesh instead of steel stirrups this ratios was 0.94, 0.93 and 0.96 for BOX 1-1, BOX2-1 and BOX3-1
 407 respectively. For the second group which used tensar wire mesh, the ratios were 0.94, 0.95 and 0.96
 408 for BOX 1-2, BOX2-2 and BOX3-2 respectively. So, the finite element analysis represents an
 409 acceptable presentation for shear stresses.
 410



411
 412

413 Fig.17: Comparison between Exp. Shear stresses and NLFE Shear stresses.
 414

415 6. CONCLUSION

416
 417

The following conclusions can be drawn:

418
 419
 420
 421
 422
 423
 424
 425
 426
 427
 428
 429
 430
 431
 432
 433

- 1- Glass fiber wire mesh and Polyethylene (tensar) wire mesh exhibited features over normal reinforcement with reinforcing steel, especially in box beams such that, it has high strength, easy to be handling cutting and shaped also has light weight with respect to steel stirrups.
- 2- Using glass fiber and tensar wire mesh instead of steel stirrups exhibit high ultimate failure load with respect to control specimen.
- 3- Tensar (Polyethylene) wire mesh has high effect in increasing load capacity, deflection, the shear stresses and cracks propagate.
- 4- The cracks propagation decreased and its number and width decreased by using glass fiber and tensar wire mesh especially in specimens with two and three layers of wire mesh.
- 5- There a reasonable agreement between experimental and numerical results obtained in form of ultimate failure load, deflection and shear stresses.
- 6- This work gives an acceptable prediction for shear stresses of box beams reinforced with glass fiber or tensar wire meshes where the obtained average ratio (V_{uNLFEA} / V_{uEXP}) was 0.938.

434
 435
 436
 437

At the end, the composite either glass fiber or tensar wire mesh in reinforcement of box sections instead of steel stirrups has a good effect in failure load, deflection, cracks propagation and shear stresses.

438
439
440
441
442
443
444
445
446
447
448
449
450
451
452
453
454
455
456
457
458
459
460
461
462
463
464
465
466
467
468

REFERENCES

- [1] ACI Committee 549. State of the art report on ferrocement. ACI 549-R97 manual of concrete practice, Detroit; 1997.
- [2] ACI Committee 549-1R-88. Guide for design construction and repair of ferrocement. ACI 549-1R-88 and 1R-93 manual of concrete practice, Detroit; 1993.
- [3] Logan, D. & Shah, S. P., Moment capacity and cracking behavior of ferrocement in flexure. ACI Journal Proceedings, 70 (12) (Dec. 1973) 799-804.
- [4] Johnston, C. D. & Mowat, D. N., Ferrocement material behavior in flexure. Journal of the Structural Division, ASCE, 100, ST10, (Oct. 1974) 2053-69.
- [5] Balaguru, P. N., Namaan, A. E. & Shah, S. P., Analysis and behavior of ferrocement in flexure. Journal of the Structural Division, ASCE, 103, ST10, (Oct. 1977) 1937-49.
- [6] Huq, S. & Pama, R. P., Ferrocement in flexure—analysis and design. Journal of Ferrocement, 8 (3) (July 1988) 169-93.
- [7] Al-Sulaimani, G. J. & Ahmad, S. F., Deflection and flexural rigidity of I- and box-beams. Journal of Ferrocement, 18, (Jan. 1988) 1-12.
- [8] Al-Sulaimani, G. J., Ahmad, S. F. & Basunbul, I. A., Study of the flexural strength of ferrocement 'flanged' beams. The Arabian Journal for Science and Engineering, 14 (1) (Jan. 1989) 33-46.
- [9] Mansur, M. A. & Ong, K. C. G., Shear strength of ferrocement beams. American Concrete Institute Structural Journal, 84 (1) (Jan.-Feb. 1987) 10-17.
- [10] El-Sayed, T.A. and Erfan, A.M., 2018. Improving shear strength of beams using ferrocement composite. Construction and Building Materials, 172, pp.608-617.
- [11] E.C.P. 203/2018, 2018, Egyptian Code of Practice: Design and Construction for Reinforced Concrete Structures, Cairo, Egypt.
- [12] ANSYS, "Engineering Analysis system user's Manual" 2005, vol. 1&2, and theoretical manual. Revision 8.0, Swanson analysis system inc., Houston, Pennsylvania.